

## Use of Few-Angstrom Radiation Imaging to Characterize Ultrabright, Multi-GeV Particle Beams

Alex H. Lumpkin and Bingxin X. Yang

*Advanced Photon Source, Argonne National Laboratory, Argonne, Illinois 60439*

(Received 24 April 1998)

We have used the 7-GeV stored positron beam at the Advanced Photon Source to approximate relevant particle beam parameters of a diffraction-limited x-ray source and to perform measurements of few- to sub-angstrom radiation. Results are based on the 198-period diagnostics undulator optimized for low-divergence radiation cones ( $\sim 2.6 \mu\text{rad}$ ) at  $\lambda \sim 0.5 \text{ \AA}$  on the fundamental and on a unique synchroscan and dual-sweep x-ray streak camera (with a few picosecond resolution) that was phase locked to the accelerator's master oscillator subharmonic. Scaling of these techniques to future sources is presented. [S0031-9007(99)08983-8]

PACS numbers: 41.60.Ap, 07.85.Qe, 41.60.Cr

The quest for diffraction-limited soft or hard x-ray sources of the future has concomitant challenges of generating and measuring ultrabright, multi-GeV particle beams [1–5]. In this Letter we report unique beam imaging experiments using few- to sub-angstrom x-ray synchrotron radiation (XSR) emitted by the beam that supports this quest. The beam conditions allowed demonstrations of capabilities in the few- $\mu\text{rad}$ , 10- $\mu\text{m}$ , and few-ps resolution regimes. Results include the measurement of a vertical beam divergence of  $3.3 \mu\text{rad}$ , the lowest value directly measured on a storage ring to date, and the first demonstrations of a unique x-ray synchroscan streak camera providing few-ps resolution while also providing spatial resolution potentially at the 10- $\mu\text{m}$  regime. We also report a novel use of the metal disk that supports the streak tube's Au strip photocathode (PC) as a lower efficiency, two-dimensional imaging detector. Although x-ray streak tubes with single fast deflections have been used for years, these are the first data taken on an accelerator or synchrotron radiation facility with the vertical sweep of the x-ray tube locked to the accelerator's rf frequency subharmonic, with sweep repetition rates of greater than 100 HMz (117.3 MHz) and with jitter less than 1 ps. The combination of low-jitter, synchronous summing of temporal profile information and improved spatial resolution in the x-ray field compared to visible light techniques extends time-resolved techniques to 10 times smaller beam sizes and to emerging pump-probe x-ray experiments on existing synchrotron light sources.

The relevance of this parameter space is that it not only covers the extended boundary of present third-generation light sources, such as the Advanced Photon Source (APS), but also reaches several of the parameter values of future light sources. Reduction of the vertical coupling (the ratio of the vertical to horizontal beam emittance) to 1%–2% and below improves the source brilliance but also results in the vertical plane's parameters approaching the values of a diffraction-limited source at  $1 \text{ \AA}$ . Such a source would have a transverse particle beam emittance,  $\varepsilon \leq \lambda/4\pi$  of about 0.01 nm rad or 10 pm rad. [This same relation-

ship applies to having adequate overlap of the particle and photon beams in a free-electron laser (FEL)]. Assuming a beta function,  $\beta = 10 \text{ m}$ , the rms beam sizes  $\sigma_{x,y} \sim 10 \mu\text{m}$  and divergences  $\sigma_{x',y'} = 1 \mu\text{rad}$  are critical values. Bunch lengths less than 1 ps (100 fs in the case of a linac-based source) are projected. Although other reports have addressed slice-emittance compensation at 40 MeV [6] and sub-ps sampling of a 50-MeV high-emittance beam with a laser [7], the present techniques deal with 7-GeV beam parameters at or within a factor of 2 to 4 of the projected future, fourth-generation light source (4GLS) designs based on linacs [8,9] or storage rings. They also support the push toward 0.1% vertical coupling in the APS storage ring.

A schematic of the experimental setup is shown in Fig. 1. The insertion device (ID) and bending magnet sources, beam lines, and instrumentation locations are indicated. The APS lattice design results in the Sector 35 ID beam being transported outboard of the next sector's first dipole magnet (a low dispersion point). A specially designed aperture assembly allows the x-ray power management from the two sources.

The basic principles for an undulator to be used for particle beam divergence measurements have been discussed elsewhere [10–12]. For an undulator with period length  $\lambda_u$ , the maximum on-axis photon flux is obtained at a wavelength,

$$\lambda_n = \frac{\lambda_u}{2n\gamma^2} \left( 1 + \frac{K^2}{2} \right), \quad (1)$$

where  $\lambda_n$  is the harmonic wavelength ( $n = 1, 3, \dots$ ),  $\gamma$  the Lorentz factor of the positron, and  $K$  the undulator parameter. At this wavelength, the rms angular width of the radiation cone is

$$\sigma_{n0} \cong \sqrt{\frac{\lambda_n}{2L}}, \quad (2)$$

where  $L = N\lambda_u$  is the length of the undulator. For a stored beam with emittance  $\varepsilon_x$  and beta function  $\beta_x$ , the

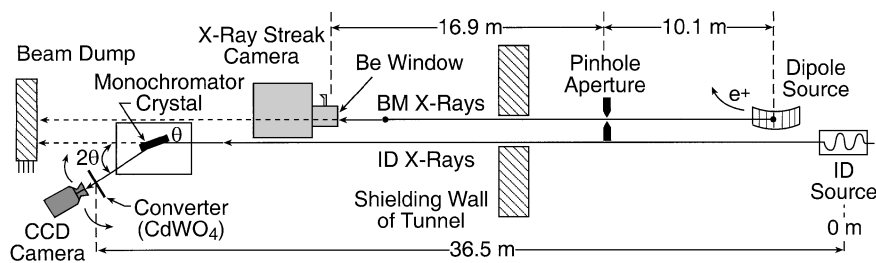


FIG. 1. Schematic of the APS diagnostics sector's sources, beam lines, and detectors. The 1.8-cm period diagnostics undulator is the ID, and one of the 80 storage ring dipole magnets is the source of x-ray synchrotron radiation. The monochromator and x-ray streak camera locations are indicated.

electron beam size and divergence are given by

$$\sigma_x \cong \sqrt{\beta_x \varepsilon_x} \quad \text{and} \quad \sigma_{x'} \cong \sqrt{\frac{\varepsilon_x}{\beta_x}}. \quad (3)$$

The photon beam profile is generally measured with a monochromator/detector combination. The rms width of this profile  $\Sigma_x$  is given by

$$\Sigma_x^2 = \sigma_x^2 + z^2 \sigma_{x'}^2 + (z - z_0)^2 \sigma_{n0}^2, \quad (4)$$

where  $z$  and  $z_0$  are distances from the  $e$ -beam waist to the detector and undulator center, respectively. The emittance can be obtained from these two latter equations,

$$\varepsilon_x = \beta_x \frac{\Sigma_x^2 - (z - z_0)^2 \sigma_{n0}^2}{\beta_x^2 + z^2}. \quad (5)$$

A similar procedure also applies to the vertical direction. For the APS diagnostics undulator [11],  $z_0 = 0.87$  m,  $\lambda_u = 1.8$  cm,  $N = 198$ , and  $\gamma = 1.4 \times 10^4$ . The undulator radiation cone is  $2.6 \mu\text{rad}$  wide in the fundamental compared to the  $8\text{-}\mu\text{rad}$  nominal vertical divergence ( $\varepsilon_y = 0.8$  nm rad and  $\beta_y = 10.1$  m). By operating at lower vertical coupling in the storage ring ( $\varepsilon_y = 0.08\text{--}0.16$  nm rad), we have produced  $\sim 3 \mu\text{rad}$  vertically divergent particle beams and measured them with a horizontally deflecting monochromator using a Si(220) or Ge(220) crystal, a  $\text{CdWO}_4$  converter crystal at  $z = 36.5$  m, and a charge-coupled device (CCD) camera.

The second series of experiments involved the first direct measurements of a multi-GeV beam's bunch length and transverse size using a unique synchroscan and dual-sweep x-ray streak camera, Hamamatsu Model C5680-36 [13] with the resolution parameter designed to APS specifications. In this case the XSR from a storage ring dipole source point is imaged by an adjustable pinhole aperture onto the streak tube PC as also shown in Fig. 1. The Au photocathode allows the detection of radiation from at least 10 eV to 10 keV and has some efficiency at energies up to 20–25 keV as shown in Fig. 2. The x-ray tube is housed in a mainframe compatible with the plug-in units of the C5680 series. For these experiments the synchroscan plug-in (Model M5675) provided the vertical (fast time) sweep, and the dual-sweep unit (Model M5679) provided the horizontal (slow time) sweep.

In the focus mode of the streak camera a Hg lamp was first used to illuminate the entire PC. We then set the x-ray apertures at  $50 \times 50 \mu\text{m}^2$  and located the image on

the gold-coated PC. We also noticed a 100 times weaker image at off  $y$ -axis positions that seemed to carry the full vertical profile information of  $\sigma_y \sim 45 \mu\text{m}$  at the source (rather than just the  $50\text{-}\mu\text{m}$  slices). Once this was done the synchroscan ranges were exercised. Three of the four were tested with x-rays. The phase adjustment and sweep speed calibrations were done using the  $z$  translator instead of an rf phase delay unit.

For the diagnostics undulator, the transverse dimensions of the monochromatic,  $\sim 26\text{-keV}$  x-ray beam,  $\Sigma_x = 870 \mu\text{m}$ , and  $\Sigma_y = 157 \mu\text{m}$ , are determined from the image shown in Fig. 3. By using the design beta functions ( $\beta_x = 14.2$  m and  $\beta_y = 10.1$  m) that were within 5% of the beam-based measurements and assuming the waist is at the design location, the horizontal ( $7.0 \pm 1.4$  nm rad) and vertical ( $0.11 \pm 0.02$  nm rad) emittances are determined from Eq. (5). These values correspond to the horizontal divergence of  $22 \pm 2 \mu\text{rad}$  and vertical divergence of  $3.3 \pm 0.9 \mu\text{rad}$ , whose contributions dominated the measured total sizes [Eq. (4)]. We have performed additional calculations and expect use of the third and fifth harmonic on-axis radiation or use of features in off-axis radiation would allow measurement resolution in the  $1\text{-}\mu\text{rad}$  regime with this device [4,10,14]. A cryocooled monochromator would probably be needed to handle the higher heat load

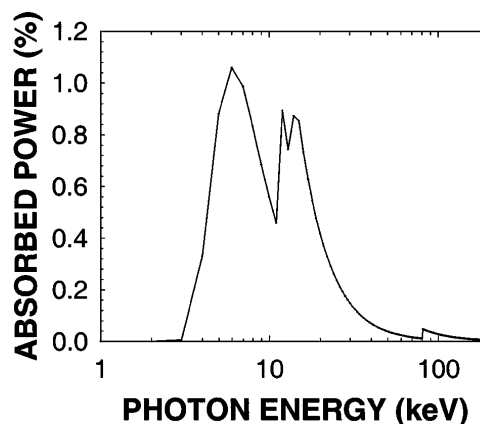


FIG. 2. An estimate of the absorbed power in percent by the Au photocathode of the x-rays spectral distribution (in keV) from the bending magnet source. The attenuation of the soft x rays by the beam line exit Be window and the x-ray tube's entrance Be window have been included.

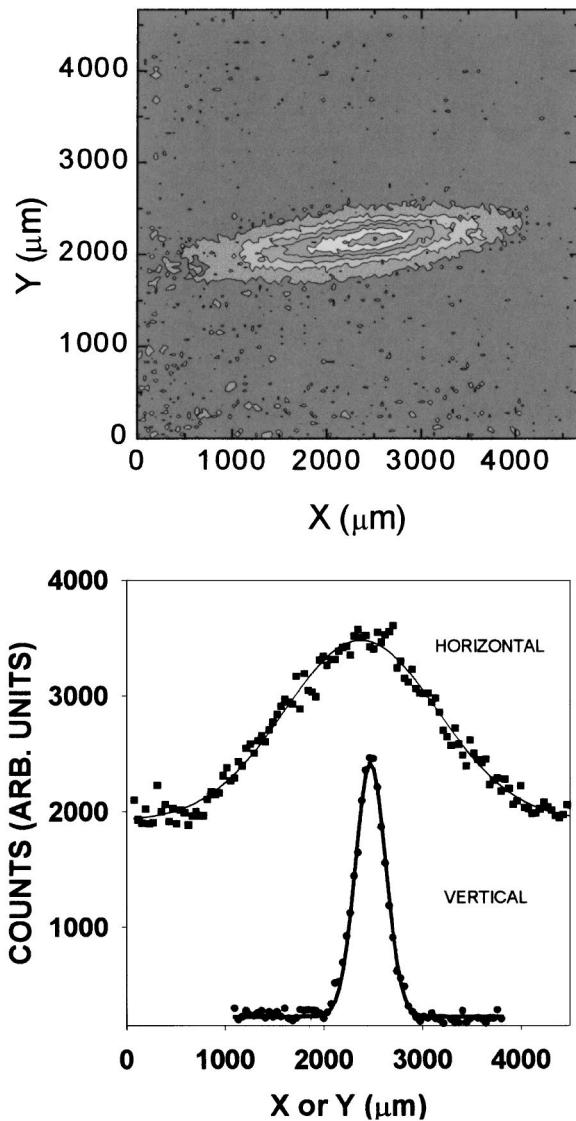


FIG. 3. A video image (top) of the sub-angstrom monochromatized output radiation from the diagnostics undulator. The particle beam's vertical divergence ( $3.3 \mu\text{rad}$ ) is the largest contribution to this spot-size profile (bottom) at a distance of 36.5 m from the source. In the other plane, the horizontal particle beam divergence was determined to be  $22 \mu\text{rad}$ .

on the crystal. The  $3.3\text{-}\mu\text{rad}$  value is one of the lowest divergences directly measured to date on a storage ring [15]. If this diagnostics undulator were operated with a 15-GeV beam, the fundamental would be at 110 keV with a cone angle of  $1.2 \mu\text{rad}$  on-axis. It seems realistic to propose that one leg of the 4GLS linac-based FEL array of beam lines should have a diagnostics undulator and a beam dump. (One straight section in a storage-ring-based device could have a dedicated device.)

It also should be noted that these measurements were done with a 30-ms integration time in the CCD camera on the 80-mA beam corresponding to an integrated charge of 2.4 mC. The ID gap was at 34 mm ( $K = 0.0076$ ) resulting in only about 0.2 W of power in the fundamen-

tal. Scaling issues include: (1) Closing the gap of this undulator to 10.5 mm (6 mm) would increase the power in the fundamental by  $3 \times 10^3$  ( $10^4$ )—the former has been measured [11] and the latter is a reasonable extrapolation, (2) using a cryocooled CCD or microchannel plate intensified camera would improve signal sensitivity by  $10^2$  to  $10^3$ , (3) reducing the horizontal emittance to  $\lambda/4\pi$  would increase the photon density by a factor of 5. This combined factor of  $10^6$  to  $10^7$  in signal and detector options should make a single pulse train measurable with  $Q \leq 1$  nC total charge. This value is close to nominal 4GLS designs. Also, a longer undulator might be used to reduce the radiation cone angle. The already low trajectory error is  $\leq 1 \mu\text{rad}$  at 7 GeV and scales down to  $<0.5 \mu\text{rad}$  at 15 GeV. Further studies with our present device are planned to address some of these points.

In Fig. 4 we show x-ray streak camera results of (a) a focus mode image from the disk PC, (b) a focus mode image from the Au strip PC, and (c) a synchroscan image with the observed bunch length of 65 ps (FWHM) or 28 ps ( $\sigma_{\text{est}}$ ). Figure 4(a) illustrates a novel 2D spatial imaging of the hard x-ray source with  $\sigma_x = 190 \mu\text{m}$  and  $\sigma_y = 45 \mu\text{m}$ . The aperture was at  $50 \times 50 \mu\text{m}^2$ . The pinhole aperture was set at  $100 \mu\text{m}$  horizontally ( $H$ ) by  $100 \mu\text{m}$  vertically ( $V$ ) with a magnification of about 1.6:1 for Figs. 4(b) and 4(c). (Data have also been obtained with apertures as small as  $10 \times 10 \mu\text{m}^2$ .) On this streak deflection range the camera rms resolution,  $\sigma_{\text{res}}$ , is determined from the focus mode image size (static spread function) to be  $\sigma_{\text{res}} \sim 4$  ps. The fastest range available is 4 times faster and implies 1 to 1.5 ps ( $\sigma$ ) resolution. The same tube was previously tested with a laser at 248 nm and due to a lower photoelectron energy distribution spread gave about 0.6-ps resolution [16,17]. These resolution numbers bound the performance for incident wavelengths from 2480 to  $\sim 1 \text{ \AA}$ . The range has an exclusion regime from 1000–200  $\text{\AA}$  due to higher absorption of these energies by the parylene substrate under the Au for this particular PC. Subsequently, the horizontal deflection was tested. Potentially, the 30-ps bunch length could be tracked over 100 ms to sub-ms ranges on the present experiment. The tube sweep speed can go down to 100 ns. Initial data are given in Ref. [18].

Although x-ray streak tubes with single fast deflections have been used for years [19], to our knowledge these are the first data taken on an accelerator or synchrotron radiation facility with the vertical sweep of the x-ray tube locked to the accelerator's rf frequency subharmonics, with repetition speeds of greater than 100 MHz (117.3 MHz), and with jitter less than 1 ps. A second, orthogonal set of deflection plates in the tube was also used for a dual-sweep demonstration down to 200  $\mu\text{s}$ , which was limited by photon intensity in the configuration. In an x-ray synchrotron radiation facility direct evaluation of the XSR may also be of interest to the user community. (This is an alternative to laser-triggered deflections in a streak tube planned for pump-probe and/or

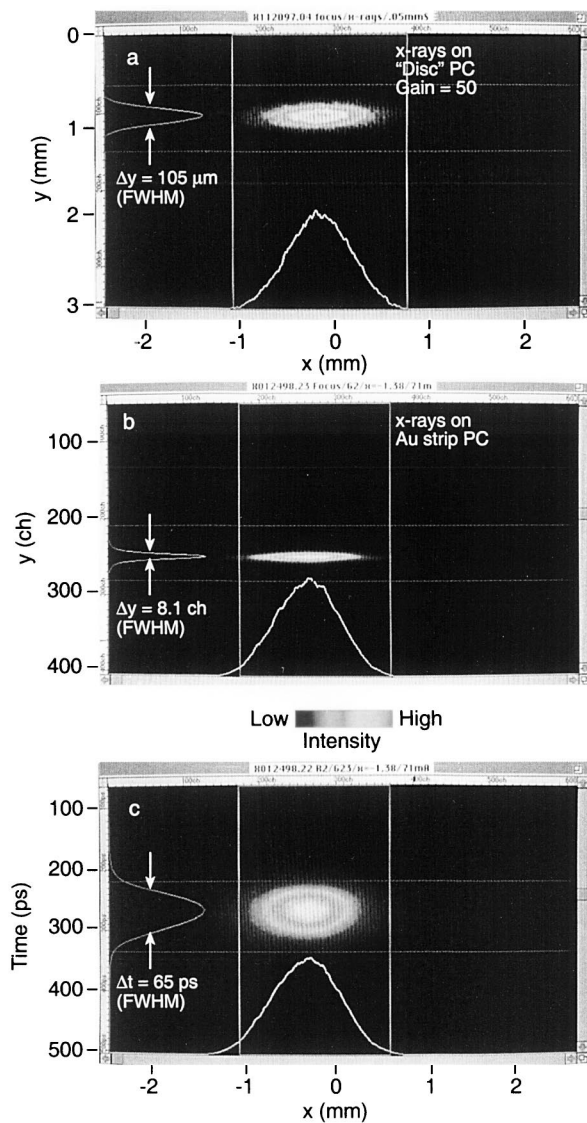


FIG. 4. X-ray streak camera images of the particle beam in (a) the focus mode on the disk PC, (b) the focus mode on the Au PC, and (c) the synchroscan streak mode on the Au PC. In the latter the bunch length ( $\sigma_t \sim 28$  ps) on the vertical axis was obtained with 4-ps temporal resolution and the horizontal size ( $\sigma_x \sim 190 \mu\text{m}$ ) with about  $15\text{-}\mu\text{m}$  spatial resolution. This synchronous sum of multiple bunches and turns is executed with low jitter by phase locking to the rf master clock's subharmonic at 117.3 MHz.

time-dependent x-ray diffraction experiments [20–22].) The use of x rays for imaging also reduces the resolution limit from diffraction effects compared to optical (visible) synchrotron radiation imaging so that some beam dynamics issues may still be addressed at smaller spot sizes.

In summary, we have demonstrated the generation and measurement of beams in APS with some beam parameters prototypical of a diffraction-limited x-ray source or 4GLS. Beam divergence of a few  $\mu\text{rad}$  in a 7-GeV beam using a scalable, diagnostics undulator, bunch length measurements of XSR with potential ps resolution, sub-ps jitter, and orthogonal time axis coverage using a unique x-ray

streak camera, and beam size measurement at the  $40\text{-}\mu\text{m}$  level were discussed. Additionally, this particular x-ray streak camera addresses the need identified for ps-domain x-ray detectors for time-resolved application experiments using 10-eV to 10-keV radiation [23]. We believe these demonstrations can provide critical data towards next-generation light source research, and these could be in the complement of diagnostics for an eventual 4GLS facility.

The authors acknowledge the support of John Galayda and Glenn Decker and the comments of Lee Teng of the APS Accelerator Systems Division. This work was supported by the U.S. Department of Energy, Office of Basic Energy Sciences, under Contract No. W-31-109-ENG-38.

- [1] *Proceedings of the Workshop on Fourth Generation Light Sources, Grenoble, France, 1996*, edited by J. LaClare (ESRF, Grenoble, 1996).
- [2] M. Poole, in (Ref. [1]), p. 69.
- [3] K.-J. Kim, *Nucl. Instrum. Methods Phys. Res., Sect. A* **393**, 147 (1997).
- [4] A. H. Lumpkin, *Nucl. Instrum. Methods Phys. Res., Sect. A* **393**, 170 (1997).
- [5] A. H. Lumpkin, in *Proceedings of the SPIE'97 FEL Challenges Conference*, SPIE Proceedings Vol. 2988 (SPIE—International Society for Optical Engineering, Bellingham, WA, 1997), p. 70.
- [6] X. Qui *et al.*, *Phys. Rev. Lett.* **76**, 3723 (1996).
- [7] W. P. Leemans *et al.*, *Phys. Rev. Lett.* **77**, 4182 (1996).
- [8] J. Arthur *et al.*, *Rev. Sci. Instrum.* **66**, 1987 (1995).
- [9] J. Rossbach, *Nucl. Instrum. Methods Phys. Res., Sect. A* **375**, 269 (1996).
- [10] Peter Ilinski *et al.*, *Proc. SPIE Int. Soc. Opt. Eng.* **2856**, 16 (1996).
- [11] B. X. Yang *et al.*, in *Proceedings of the 1997 Particle Accelerator Conference, Vancouver, BC, Canada, 1997* (IEEE, Piscataway, 1998), Vol. 2, p. 2207.
- [12] E. Tarazona and P. Elleaume, *Rev. Sci. Instrum.* **66**, 1974 (1995).
- [13] Hamamatsu Photonics, C5680 Universal Streak Camera Data Sheet, May 1993.
- [14] P. Heiman *et al.*, *Rev. Sci. Instrum.* **66**, 1885 (1995).
- [15] P. Elleaume, C. Fortgang, C. Penel, and E. Tarazona, *J. Synchrotron Radiat.* **2**, 209 (1995).
- [16] A. H. Lumpkin, B. Yang, W. Gai, and W. Cieslik, in *Proceedings of the 1995 PAC, Dallas, Texas* (IEEE, Piscataway, 1996), Vol. 4, p. 2476.
- [17] A. Lumpkin, *Nucl. Instrum. Methods Phys. Res., Sect. A* **375**, 460 (1996).
- [18] A. H. Lumpkin and B. X. Yang, in *Proceedings of BIW'98, SLAC, 1998* (AIP, Woodbury, 1998), No. 451, p. 214.
- [19] G. Stradling, *Proc. SPIE Int. Soc. Opt. Eng.* **1032**, 194 (1988).
- [20] Z. Chang *et al.*, *Appl. Phys. Lett.* **69**, 133 (1996).
- [21] M. Wulff *et al.*, *Nucl. Instrum. Methods Phys. Res., Sect. A* **398**, 69 (1997).
- [22] J. Larsson *et al.*, *Opt. Lett.* **22**, 1012 (1997).
- [23] M. Knotek, in *Proceedings of the Workshop on Scientific Opportunities for Fourth-Generation Light Sources*, Argonne National Laboratory, 1997 (unpublished).